Assessing a Shift of Glucose Biotransformation by LC-MS/MS-based Metabolome Analysis in Carbon Monoxide-Exposed Cells

Naoharu Takano, Takehiro Yamamoto, Takeshi Adachi, and Makoto Suematsu

Abstract Carbon monoxide (CO) is the stress-inducible gas generated by heme oxygenase (HO). Although the HO/CO system appears to contribute to cell protection and tissue repair under stress conditions, its mode of actions remains largely unknown. We hypothesized that CO might alter the cellular energetic conditions and thereby modulate oxygen metabolism. To examine this hypothesis, we attempted to establish a method to follow the global flux of ^{13}C-glucose in the cells using metabolomic approaches with liquid chromatography-mass spectrometry (LC-MS/MS). The human monoblastic leukemia cell line U937 was exposed to the CO-releasing molecule (CORM). The CO exposure attenuated the conversion of the mass-labeled glucose to its downstream metabolites, while significantly stimulating its conversion to those for pentose phosphate pathway, suggesting roles of stress-inducible CO in a shift of glucose biotransformation.

1 Introduction

Within the cells, glucose is mainly catalyzed through glycolysis and pentose phosphate pathway. Such a utilization of glucose is necessary for cellular adaptation against stressors. For examples, hypoxia induces a transcriptional factor, hypoxia inducible factor-1 (HIF-1), which induces GLUT-1, GAPDH, PDK-1, and LDH [1], and promotes anaerobic glycolysis to adapt hypoxia. Since hypoxia causes an induction of heme oxygenase [2, 3], the CO-producing enzyme, it is not unreasonable to hypothesize that the gas might also change the biotransformation of glucose. To measure the global picture of glucose utilization, we have herein established the flux analysis with ^{13}C-labeled glucose using

M. Suematsu (✉)
Department of Biochemistry & Integrative Medical Biology, School of Medicine, Keio University, Tokyo, 160-8582, Japan
e-mail: msuem@sc.itc.keio.ac.jp

E. Takahashi, D.F. Bruley (eds.), *Oxygen Transport to Tissue XXXI*, Advances in Experimental Medicine and Biology 662,
DOI 10.1007/978-1-4419-1241-1_14,

LC-MS/MS. Using this methodology, we aimed to examine the effects of CO on glucose utilization through the fluxome analysis.

2 Materials and Methods

2.1 Materials and Extraction of Metabolites

DHAP, 2-deoxy-G6P, Gal1P, GA3P, 3PG, and 6PG were purchased from Sigma. Fru1, 6P2, Ribo5P, and Xylu5P were purchased from Fluka. Fru6P, Glu1P, Glu6P, Pyr, PEP, were purchased from Wako. Lac was purchased from Tokyo Kasei Kogyo. Sed7P was purchased from GLYCOTEAM GmbH. CORM (Tricarbonyldichlororuthenium(II) dimer) and ruthenium (III) chloride (Ru) were purchased from Aldrich. U937 cells were cultured with RPMI-1640 medium supplemented with 10% FBS, penicillin and streptomycin, and grown in a CO_2 incubator. U937 cells were plated at 5×10^6 cells/10 cm dish and cultured around 14 h. Then the cells were treated with 100 μM CORM or Ru as a control for 30 min. After the CORM or Ru treatment, medium was exchanged to glucose-free RPMI-1640 supplemented with 10% FBS, penicillin and streptomycin, and added $^{13}C_6$-glucose at 2000 mg/L. After the addition of $^{13}C_6$-glucose containing medium, cells were left for 5 min in the CO_2 incubator and immediately centrifuged to collect them at 1,500 rpm for 2 min. Then cells were washed with PBS(–) once. Collected cells were immediately frozen in liquid N_2 and stored at –80°C until extraction. 400 μl methanol containing internal standard (IS) (2-deoxy-glucose-6P: 0.3 μM) were added to harvested cells and voltexed. Then, 200 μL water was added and mixed for 30 min. After the addition of 400 μL chloroform and voltexed, centrifuged at 14,000×*g* for 30 min. Supernatant were filtrated with 5 kDa cut-off filter and dried with Speed-Vac. Dried samples were stored at –80°C till LC-MS/MS analysis.

2.2 LC-MS/MS

LC-MS/MS analysis was performed as previously reported with some modifications [4, 5]. Chromatographic separations were carried out on Synergi Hydro-RP (C18) column (150 × 2.0 mm, 4 μm, 80 Å, phenomenex). The chromato-graphic system was an Agilent 1100 series binary HPLC system (Agilent Technologies). Separations were performed under gradient conditions as described in Table 1. Column temperature was set to 40°C. Mobile phases consisted of 15 mM acetic acid/10 mM tributylamine/H_2O (A) and 100% Methanol (B).

Mass spectrometry analysis was carried out on Applied Biosystems/API 3000 equipped with a TurboIon spray source. The MS was operated in the negative ion and multiple reactions monitoring (MRM) mode. Single analyte standard dissolved in a 10 mM acetic acid was infused at a flow rate of 5 μL/min

Table 1 Gradient profile

Period	Step	Total time (min)	Flow rate (μL/min)	A(%)	B(%)
1	0	10.0	200	99	1
1	1	10.0	200	99	1
1	2	25.0	200	80	20
2	3	30.0	200	80	20
2	4	30.1	200	65	35
2	5	35.0	200	65	35
2	6	40.0	200	40	60
2	7	45.0	200	40	60
2	8	45.1	200	10	90
2	9	55.0	200	10	90

Column was equilibrated in step 0 for 10 min and MRM scan was separated in 2 periods at step 3

for tuning compound dependent MS parameters. These parameters were as follows: ionspray voltage −4000 V, nebulizer gas (NEB) 14, curtain gas (GUS) 14, auxiliary gas temperature (TEM) 400, and collision gas (CAD) 4. MS parameters for each metabolite are given in Table 2. Extracted metabolites were diluted with 50 μL of H_2O and the injected volume was 10 μL. Standard samples (1 μM) and extracted metabolites from cultured cells were measured by LC-MS/MS and detected peaks were compared. Areas of each metabolite were calculated and divided by IS peak area.

3 Results

3.1 Measurement of ^{13}C-Labeled Metabolites by LC-MS/MS

To assess the effect of carbon monoxide on glucose metabolism, we tried to establish a method for measuring the global flux of $^{13}C_6$-labeled glucose by modifying the method previously reported by Luo et al. [4, 5]. First, we measured standard samples and confirmed the detection of each metabolite. Detected peaks of each standard are shown in Fig. 1. Sed7P, Ribo5P, Ribu5P, Xylu5P, Glu6P, Fru6P, Glu1P, Gal1P, GA3P, DHAP, Pyr, Lac and 2-deoxy-G6P were detected in period 1 and 6PG, Fru1, 6P2, 3PG, and PEP were detected in period 2. MS scan for Glu1P/Gal1P and Glu6P/Fru6P detected all other metabolites but in lower sensitivity (Fig. 1d). Next, we confirmed the detection of ^{13}C-labeled metabolites. We measured the cells cultured without $^{13}C_6$-glucose as a negative control and confirmed that they did not give peaks of ^{13}C-labeled metabolites (data not shown). Then, we measured the cells cultured with $^{13}C_6$-glucose and checked the overlap of signals derived from ^{13}C-labeled metabolites and non-labeled metabolites (Fig. 1). With these results, we confirmed that metabolites derived from $^{13}C_6$-glucose were measured correctly.

Table 2 MS parameters

Compound	Q1(12C)	Q1(13C)	Q3(12C)	Q3(12C)	DP	FP	EP	CE	CXP
Glu1P/Gal1P	258.744	264.744	78.95	78.95	−41	−300	−10	−40	−5
Glu6P/Fru6P	258.745	264.744	97.15	97.15	−36	−36	−10	−24	−5
GA3P/DHAP	168.751	171.75	97.15	97.15	−41	−330	−10	−14	−5
Pyr	86.852	89.8	43.25	45.3	−31	−330	−10	−12	−1
Lac	88.826	91.8	43.25	45.3	−26	−240	−10	−18	−1
Rbio5P/Ribu5P/Xylu5P	228.714	233.714	97.15	97.15	−31	−230	−10	−18	−5
Sed7P	288.817	295.817	97.15	97.15	−41	−330	−10	−28	−5
2-deoxy-G6P	242.85		97.15		−86	−250	−10	−22	−5
Fru1,6P2	338.4	344.4	97.15	97.15	−36	−260	−10	−30	−7
3PG	184.782	187.782	97.15	97.15	−31	−260	−10	−22	−5
PEP	166.758	169.758	79.05	79.05	−21	−220	−10	−16	−1
6PG	274.826	280.826	97.15	97.15	−21	−230	−10	−24	−5

Abbreviations: Glu1P: glucose-1-phosphate; Gal1P: galactose-1-phosphate; Glu6P: glucose-6-phosphate; Fru6P: frucotse-6-phosphate; GA3P: glyceraldehyde-3-phosphate; DHAP: dihydroxy-acetone-phosphate; Pyr: pyruvate; Lac: lactate; Ribo5P: ribose-5-phosphate; Ribu5P: ribulose-5-phosphate; Xylu5P: xylulose-5-phosphate; Sed7P: sedheptulose-7-phosphate; 2-deoxy-G6P: 2-deoxy-glucose-6-phosphate; Fru1,6P2: fructose-1,6-bisphosphate; 3PG: 3-phospho-glycerate; PEP: phosphoenolpyruvate; 6PG: 6-phospho-gluconate.

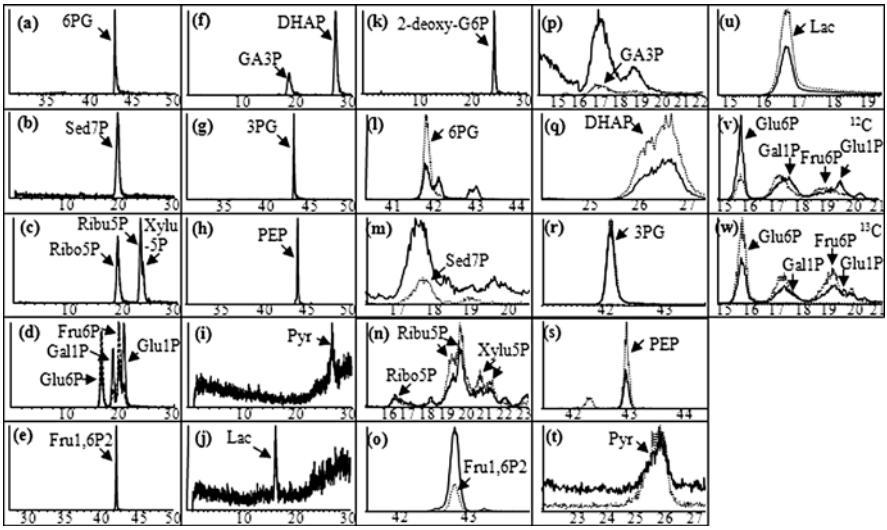

Fig. 1 Chromatograms of standard samples (**a–k**) and metabolites in extracted samples (**l–w**). Each chromatogram shows the result of LS-MS/MS analysis of 1 μM standard samples (**a–k**). Retention times are shown at the bottom of each chromatogram. Arrows (**a–k**) indicate peaks of detected standard samples. (**d**) Solid line indicates MS scan of Gal1P/Glu1P and dashed line indicates MS scan of Glu6P/Fru6P. Solid lines indicate [^{12}C] metabolites and dashed lines indicate [^{13}C] metabolites (**l–u**). Solid line indicates MS scan of Gal1P/Glu1P and dashed line indicates MS scan of Glu6P/Fru6P (v, w). [^{12}C] metabolites and [^{13}C] metabolites are shown in (v) and (w), respectively. Arrows indicate detected [^{13}C] labeled in each metabolite (**l–w**)

3.2 Effect of CO on Glucose Metabolism

To assess the effect of CO on glucose metabolism, we measured and compared the global flux of $^{13}C_6$-glucose between CORM treated and Ru treated U937 cells (Fig. 2). This result shows that the amount of 6PG, Xylu5P was significantly increased and Sed7P and Ribu5P were modestly increased by CORM treatment, they were located on PPP. On the other hand, GA3P and 3PG were significantly decreased and PEP was modestly decreased by CORM treatment, they were located on the glycolytic pathway. These results indicate that CO suppressed flux to the glycolytic pathway, and increased flux to PPP.

4 Discussion

CO is produced by HO in response to a variety of stress, and is known to contribute to cell protection [2, 3]. In this report, we showed that CO worked as a putative metabolic regulator for glucose biotransformation, although the mechanisms remain unknown. Because activation of PPP produces NADPH by G6PD [6], CO might regulate redox conditions within cells, functioning

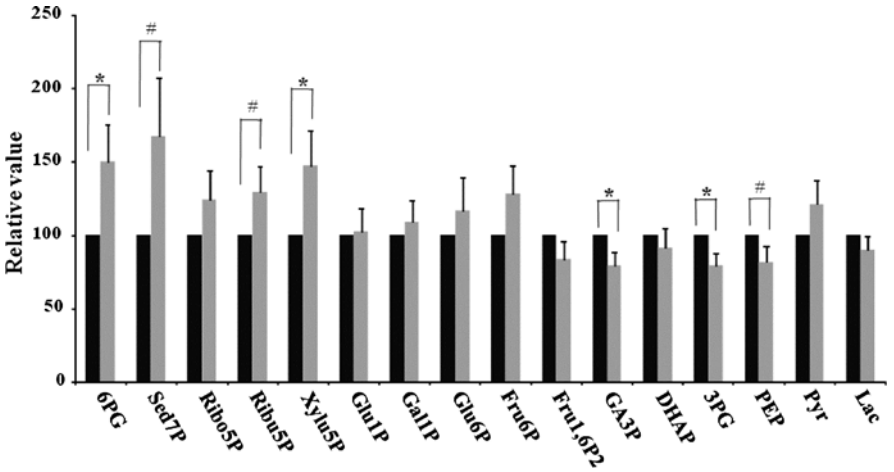

Fig. 2 Measurement of each [^{13}C] metabolite in Ru (*black bars*) or CORM (*gray bars*) treated U937 cells. Each value was calculated as relative value when the amount of each metabolite in Ru-treated cells was defined as 100. Bars indicate means ± S.E , $*P < 0.05$, $\#P < 0.07$, $n = 7$

against stresses. On the other hand, CO appears to suppress glycolysis. Since the cells were viable under the current experimental conditions, alternative mechanisms for cellular energetic to maintain ATP in the CO-exposed cells should be further examined. Collectively, the current study provided a useful method to follow the fate of glucose in different types of cells including not only those of mammals but of microorganisms which are exposed to varied stress conditions.

Acknowledgments This study is supported in part by Grant-in-Aid for Creative Scientific Research from MEXT, Grant-in-Aid for Young Scientists (B) from MEXT, Health and Labor Science Research Grant on Advanced Medical Technology from MHLW, and Scientific Frontier Research Grant from MEXT.

References

1. Airley RE, and Mobasheri A. Hypoxic regulation of glucose transport, anaerobic metabolism and angiogenesis in cancer: novel pathways and targets for anticancer therapeutics. Chemotherapy. 53(4), 233–256 (2007).
2. Suematsu M, and Ishimura Y. The heme oxygenase-carbon monoxide system: a regulator of hepatobiliary function. Hepatology. 31(1), 3–6 (2000).
3. Kyokane T, Norimizu S, Taniai H, Yamaguchi T, Takeoka S, Tsuchida E, Naito M, Nimura Y, Ishimura Y, and Suematsu M. Carbon monoxide from heme catabolism protects against hepatobiliary dysfunction in endotoxin-treated rat liver. Gastroenterology.120(5), 1227–1240 (2001).
4. Luo B, Groenke K, Takors R, Wandrey C, and Oldiges M. Simultaneous determination of multiple intracellular metabolites in glycolysis, pentose phosphate pathway and

tricarboxylic acid cycle by liquid chromatography-mass spectrometry. J. Chromato. A. 1147, 153–164 (2007).
5. Tian J, Bryk R, Itoh M, Suematsu M, and Nathan C. Variant tricarboxylic acid cycle in My-cobacterium tuberculosis: identification of alpha-ketoglutarate decarboxylase. Proc Natl Acad Sci USA. 102(30), 10670–10675 (2005).
6. Ho HY, Cheng ML, and Chiu DT. Glucose-6-phosphate dehydrogenase – from oxidative stress to cellular functions and degenerative diseases. Redox Rep. 12(3), 109–118 (2007).